Low temperature behaviour of quantum paraelectric $SrTiO_3$ weakly doped with Ca^{2+} impurities

2001 J. Phys.: Condens. Matter 13 5957

(http://iopscience.iop.org/0953-8984/13/26/311)

INSTITUTE OF PHYSICS PUBLISHING JOURNAL OF PHYSICS: CONDENSED MATTER

J. Phys.: Condens. Matter **13** (2001) 5957–5970 www.iop.org/Journals/cm PII: S0953-8984(01)23156-7

Low temperature behaviour of quantum paraelectric $SrTiO_3$ weakly doped with Ca^{2+} impurities

Serguei A Prosandeev[1], Wolfgang Kleemann[2] and Jan Dec[3]

[1] Physics Department, Rostov State University, 344090 Rostov-on-Don, Russia
[2] Laboratorium für Angewandte Physik, Gerhard-Mercator-Universität Duisburg, D-47048 Duisburg, Germany
[3] Institute of Physics, University of Silesia, PL 40-007 Katowice, Poland

E-mail: wolfgang@kleemann.uni-duisburg.de

Received 21 March 2001, in final form 27 April 2001

Abstract

The influence of point defects on the dielectric susceptibility as observed on $Sr_{1-x}Ca_xTiO_3$ with $x \leqslant 0.007$ is described within the framework of two microscopic models. While the 'soft impurity oscillator model' readily explains the induced lattice softening at low concentrations, an adequate description of the ferroelectric instability and nonlinear dielectric behaviour requires dominance of a 'mode coupling model' at higher concentrations. It involves the soft-mode and tunnelling ions, whose appearance is explained within a percolation approach.

1. Introduction

Quantum paraelectrics like $SrTiO_3$ and $KTaO_3$ are known to remain in the paraelectric state even at zero temperature as a consequence of zero-point quantum vibrations of their ions [1]. These vibrations suppress the ferroelectric phase transition although, from the point of view of classic thermodynamics, it should appear at $T = 0$. It is known that uniaxial stress [2] or small additions of impurities [3–5] can trigger the phase transition into a long-range ordered state. In the present paper we consider the case of solid solutions of $Sr_{1-x}Ca_xTiO_3$, $x \ll 1$ (SCT for short). The dielectric properties of these solid solutions have been studied in several papers [3–5]. In the low-x limit it was found that the Ca impurities drastically increase the dielectric susceptibility, although the phase transition does not yet appear. This feature is satisfactorily explained within the framework of a 'soft impurity oscillator model', which will be developed in this paper first.

The obvious failure of this model to describe correctly the ferroelectric instability and the electric field dependence of the dielectric susceptibility [5] then forces us to extend our treatment towards a 'mode coupling model', which involves the soft-mode and tunnelling polar impurities. When fitting this model to experimental data, very large electric dipole moments are encountered, which cannot be attributed to single Ca^{2+} impurities. Obviously clustering

takes place, which is described within a percolation approach by considering random site distribution and temperature dependent correlation radii.

It will be shown that the two models proposed in this paper are not mutually exclusive. On the contrary, they are complementary in the following sense. Isolated Ca^{2+} ions substituted at Sr^{2+} sites at low concentrations probably lack dipolar properties to a large extent, since their off-centrality is very small in view of the minute differences in ionic radii. However, at high enough Ca^{2+} concentrations interactions between the impurities break their spherical symmetry. Finite dipole moments are thus induced, which give rise to mode coupling effects.

2. Theory

2.1. Soft impurity oscillator model

We start with the standard Hamiltonian [6] describing a set of linearly coupled harmonic oscillators

$$H_{harm} = \frac{1}{2}\sum_{ni} M_i\omega_i^2 x_{ni}^2 + \frac{1}{2}\sum_{ni\neq mj} \upsilon_{ni,mj} x_{ni} x_{mj}. \tag{1}$$

Here ω_i, x_{ni} and M_i are the eigenfrequency, atomic displacement and atomic mass for the ith ion in the unit cell, respectively. $\upsilon_{ni,mj}$ is the spring constant coupling the displacements x_{ni} and x_{mj} of different ions. After finding the eigenvalues of this Hamiltonian, ω_{ki}, it can be written as

$$H_{harm} = \frac{1}{2}\sum_{ki} \omega_{ki}^2 y_{ki} y_{-ki}. \tag{2}$$

Here y_{ki} is the normal displacement in the ith vibration mode. We add to this Hamiltonian an anharmonic part, which is responsible for the temperature dependence of the soft mode

$$H = H_{harm} + \frac{1}{4}\sum_{\boldsymbol{k}_1 i_1, \boldsymbol{k}_2 i_2, \boldsymbol{k}_3 i_3, \boldsymbol{k}_4 i_4} V(\boldsymbol{k}_1, \boldsymbol{k}_2, \boldsymbol{k}_3, \boldsymbol{k}_4) x_{\boldsymbol{k}_1 i_1} x_{\boldsymbol{k}_2 i_2} x_{\boldsymbol{k}_3 i_3} x_{\boldsymbol{k}_4 i_4} \tag{3}$$

In the self-consistent phonon approximation [7] the free energy density corresponding to this Hamiltonian can be represented in the form of a Landau–Devonshire expansion,

$$F = F_0 + \tfrac{1}{2}\alpha(T)P^2 + \tfrac{1}{4}bP^4 \tag{4}$$

where

$$\alpha(T) = \alpha_0 + A\sum_{ki} \frac{c_{ki}^2}{\omega_{ki}}\left(\coth\frac{\hbar\omega_{ki}}{2k_BT} - 1\right). \tag{5}$$

Here α_0 is determined by the harmonic contribution to the Hamiltonian, A is a constant which is proportional to the anharmonicity constant and c_{ki}^2 is the weight of the critical mode in the phonon mode with frequency ω_{ki} referring to the wavevector $\boldsymbol{k}$ and the branch i. Note that in equation (4) only electric non-linearity terms are taken into account, while terms connected with stresses are neglected.

So far we have described the Hamiltonian of the perfect crystal. In a crystal with imperfections, e.g. SCT, we assume that the point defects have modified squared eigenfrequencies, say ω_{Ca}^2 instead of ω_{Sr}^2. The difference between these squared frequencies will be called $\Xi = \omega_{Sr}^2 - \omega_{Ca}^2$. Thus the corresponding change of the free energy can be estimated from the first order correction

$$\begin{aligned}\Delta F = \langle\Delta H\rangle &= -\frac{1}{2}n_1\Xi\langle x_{Ca}^2\rangle = -\frac{1}{2}n_1\Xi\sigma_{Ca}(T) - \frac{1}{2}n_1\Xi\langle x_{Ca}\rangle^2 \\ &= \Delta F_0(T) - \frac{1}{2}n_1\frac{\Xi c_{Ca}^2}{z_c^2}P^2\end{aligned} \tag{6}$$

where $\sigma(T)$ is the variance of the Ca coordinate; n_1 is the volume impurity concentration; c_{Ca}^2 is the weight of the Ca^{2+} ion in the soft mode and z_c is the charge corresponding to the critical mode. Corrections of higher than quadratic order are neglected, since fluctuations of the polarization are small in the paraelectric phase. This is e.g. evidenced by the parallel T dependence of the susceptibility for $x = 0$ and 0.002 (figure 2). Finally, one obtains the following form of the free energy:

$$F' = F_0' + \tfrac{1}{2}(\alpha(T) - \Lambda n_1)P^2 + \tfrac{1}{4}bP^4 - EP \tag{7}$$

where $F_0' = F_0 + \Delta F_0$ and $\Lambda = \Xi c_{Ca}^2/z_c^2$. It is seen that the impurity contribution to the free energy varies linearly with n_1. The coefficient Λ, which couples the squared polarization to the concentration of the impurities, is temperature independent. This result corresponds to a previous phenomenological consideration of Hayward and Salje [8].

Experimentally the temperature and concentration dependence of the free energy can be obtained from measurements of the dielectric susceptibility data, which should be compared to that calculated from equation (7),

$$\chi = \frac{1}{\varepsilon_0}\frac{\partial P}{\partial E} = \frac{1}{\varepsilon_0}\frac{1}{\alpha(T) + 3bP^2 - \Lambda n_1}. \tag{8}$$

It is seen from this expression that the impurities can give rise to a divergence of the dielectric susceptibility and, hence, to a phase transition. We should notice, however, that the impurities can no longer be considered as being non-interacting in the vicinity of the phase transition. Hence, equation (8) will hold only when the interaction radius between the impurities is smaller than their average distance.

In order to evidence, as suggested by equation (5), that the measured dielectric susceptibility is really related to the soft mode frequency we have plotted the dielectric susceptibility [9] together with the reverse squared soft mode frequency taken from hyper-Raman spectra [10] of $SrTiO_3$ (figure 1). It is seen that these two curves have the same shape thus justifying our assumptions. It should be noticed that, owing to the tetragonal symmetry of $SrTiO_3$ at $T < T_0 = 105$ K [1], exclusively the susceptibility within the easy ab-plane, $\chi_{11} = \chi_{22} = \chi$, is considered. Assuming equal coupling A, of all lattice modes to $\alpha(T)$ in equation (5), the susceptibility being determined by the squared inverse soft mode frequencies [11] will refer to the optic branches with lowest energy, A_{1u} and E_u. Hence, when plotting the graph we used the expression $\overline{\omega}^{-2} = (\omega_1^{-2} + 2\omega_2^{-2})/3$ in order to describe the dielectric response of the lattice rather than the average $\overline{\omega}^2 = (\omega_1^2 + 2\omega_2^2)/3$ as proposed previously [10]. Here ω_1^2 and ω_2^2 correspond to the A_{1u} and E_u vibrational frequencies, respectively.

Figure 2 shows the reverse dielectric susceptibility of pure $SrTiO_3$ and SCT with $x = 0.002$ [5, 9]. The fact that the curves are nearly parallel confirms the predicted dependence of the susceptibility on the impurity concentration at small concentration.

In order to study the concentrational phase diagram one can use the approximate expressions [12]

$$\alpha(T) = \begin{cases} A(T^2 - T_{c0}^2) & \theta > T > T_c \\ B(T - T_0) & T > \theta \end{cases} \tag{9}$$

which, in turn, imply the renormalized Curie temperature to depend on n_1 as

$$T_c = \begin{cases} C\sqrt{n_1 - n_{c1}} & \theta > T_c \\ D(n_1 - n_{c0}) & T_C > \theta. \end{cases} \tag{10}$$

Here n_{c1} and n_{c0} are the critical concentrations in the quantum and in the classical approaches, respectively, where $n_{c1} > n_{c0}$. θ is the temperature at which the classical behaviour is

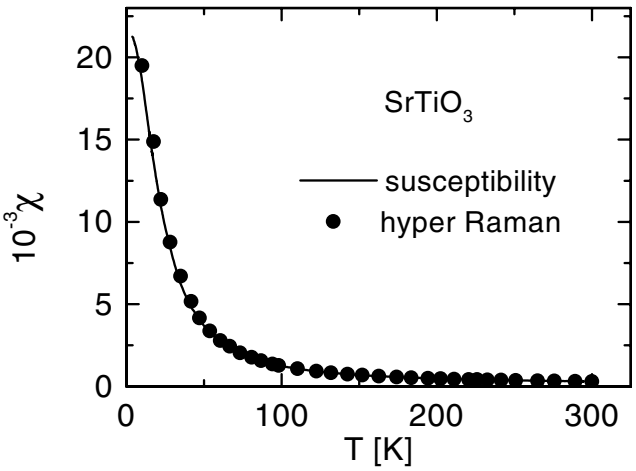

Figure 1. Temperature dependence of the in-plane dielectric susceptibility [9] (solid line) and squared inverse soft-mode frequency, $1/\overline{\omega}^2$ [10], of pure $SrTiO_3$ (solid circles; normalized to the χ' data).

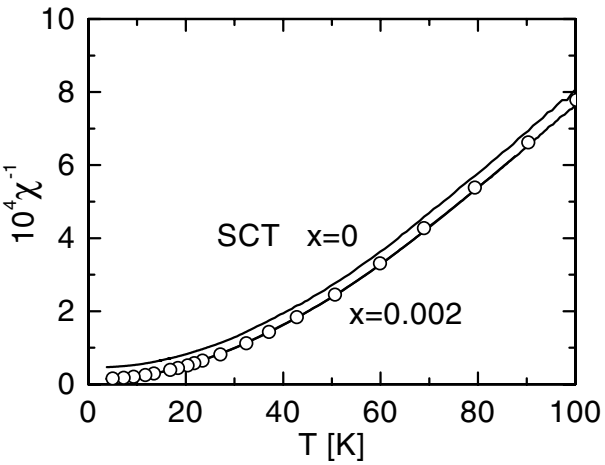

Figure 2. Temperature dependence of the inverse in-plane dielectric susceptibility [9] of pure ($x = 0$) and Ca doped ($x = 0.002$) single domained tetragonal $SrTiO_3$. Open circles denote parallel shifted $x = 0$ data best-fitted to the $x = 0.002$ ones.

substituted by the quantum mechanical one, while T_{c0} and T_0 are the critical and the extrapolated Curie temperatures, respectively. Such a transition between these two regimes has indeed been observed in experiments on SCT in the low-concentration limit, $x \gtrsim 0.002$ [3].

The above model of soft impurity oscillators can also explain the influence of the oxygen vacancies on the phonon spectrum. Due to the well known [13] high polarizability of O^{2-}, loss of an oxygen ion from the lattice implies a *decrease* of the polarizability for the corresponding site. Again, equation (8) will hold in this case when using a negative coupling constant, $\Lambda < 0$. Thus the oxygen vacancies decrease the dielectric susceptibility while hardening the soft mode. This finding is in good agreement with the experimental data on Raman spectroscopy applied to reduced $KTaO_3$ [14], recent experimental findings in $SrTiO_3$ thin films [15] as well as with

theoretical studies considering stresses appearing at the oxygen vacancies [16]. It should be remarked that polarons might contribute to χ as well [17], if the vacancies are not completely compensated by acceptors. Fortunately, polarons are usually recognized by changes of the sample's optical absorption (colour), luminescence and electric resistivity, all of which are assumed negligible in SCT.

A crucial test of the validity of equation (8) is provided by its comparison with the field dependence of the susceptibility, χ against E at constant T. To this end we have to insert the field-induced polarization

$$P = (((a/3b)^3 + (E/2b)^2)^{1/2} + E/2b)^{1/3} - (((a/3b)^3 + (E/2b)^2)^{1/2} - E/2b)^{1/3} \tag{11}$$

as calculated from the equation of state

$$E = aP + bP^3 \tag{12}$$

where $a = \alpha(T) - \Lambda n_1$.

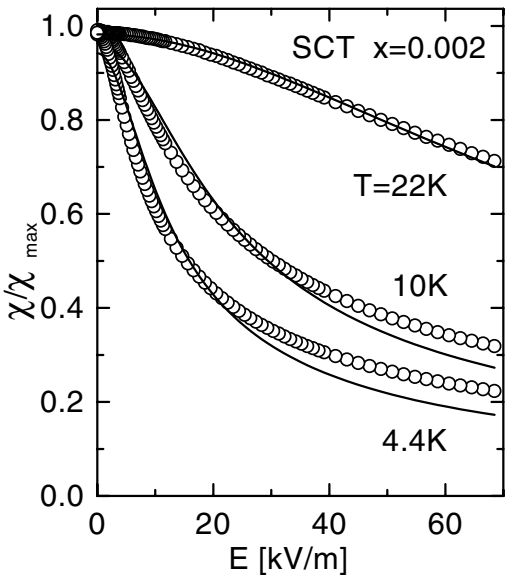

Figure 3. Normalized electric field dependences for various temperatures of the in-plane dielectric susceptibility [9] of SCT with $x = 0.002$ compared to best fits to equation (8) after insertion of equation (11).

Figure 3 shows experimental data obtained on SCT with $x = 0.002$ at $T = 4.4$, 10 and 22 K together with best fits to equation (8) after insertion of equation (11). It is seen that these fits are quite poor for $T \leqslant 10$ K, where they fail to model the flat tails of $\chi'(E)$ at fields exceeding $E \approx 20$ kV m^{-1}. Inspection of the shape of these isotherms suggests them to contain two different contributions, a rapidly decaying one at low E values and second one saturating only at very high fields. Previously [4, 18] we described such behaviour empirically by superimposing cluster contributions with rapidly saturating *Langevin*-type field response to a conventional non-linear lattice background. This idea is revisited in section 2.2 within the framework of a mode coupling approach, the principle of which was outlined previously [5, 18].

2.2. Mode coupling model

Let us consider a Hamiltonian describing the critical mode of the host lattice and a set of tunnelling ions, which mimic those Ca^{2+} ions possessing a local dipole moment:

$$H = \frac{1}{2}\sum_{k}\omega_k^2 y_k y_{-k} + \frac{1}{4}\sum_{k_1,k_2,k_3,k_4} V(\boldsymbol{k}_1,\boldsymbol{k}_2,\boldsymbol{k}_3,\boldsymbol{k}_4) y_{k_1} y_{k_2} y_{k_3} y_{k_4}$$
$$-E\sum_i z_i x_i - n_2\Omega\sum_i S_i^x - \frac{1}{2}n_2\sum_{i\neq j} J_{ij} S_i^z S_j^z$$
$$-n_2\sum_{ij}\lambda_{ij} x_i S_j^z - 2\mu n_2 E\sum_i S_i^z. \tag{13}$$

In this expression the impurities with volume concentration n_2 are described within the framework of the transverse Ising model [11] (by using pseudo-spin components $S_i^{x,z}$, spin–spin interaction $J_0 = \sum_j J_{ij}$, the tunnelling integral Ω and the electric dipole moment associated with the spins μ) and bilinear coupling (strength $\lambda = \sum_j \lambda_{ij}$) between the soft mode displacement x_i with effective charges z_i and pseudo-spin component S_j^z [5, 18].

At first the displacements and spin coordinates are considered to be mutually independent and then we introduce the interaction term from a first order perturbation approach. The free energy expansions for the polarization referring to the soft mode and to the dipoles, F_{sm} and F_{dip}, respectively, are

$$F_{sm} = F_0 + \tfrac{1}{2}\alpha(T)P_0^2 + \tfrac{1}{4}bP_0^4 - P_0(E + n_2\lambda\langle S^z\rangle) \tag{14}$$

$$F_{dip} = -k_B T \ln\left[2\cosh\left(\frac{W}{2k_B T}\right)\right] + \frac{1}{2}J_0\langle S^z\rangle^2 \tag{15}$$

where $W = \sqrt{\Omega^2 + W_z^2}$ and $W_z = 2\mu E + J_0\langle S^z\rangle + \lambda P_0$. Note that $\alpha(T)$ as defined by equation (5) has the same meaning as in the soft mode model of section 2.1. It designates the reverse dielectric permittivity of the host lattice, which refers to the unperturbed crystal without point defects. While in the soft mode picture the s-type impurities simply subtract a constant from $\alpha(T)$, the dipolar impurities subtract a constant divided by T. P_0 is the part of the polarization referring to the soft mode, and $P_1 = 2\mu n_2\langle S^z\rangle$ is that due to the tunnelling ions. In equation (15) the average field is replaced by the local field at the impurity sites, which accounts for the interaction of the impurities with the average polarization. For similar reasons, the average field in the free energy describing the soft mode, equation (14), is substituted by the local field produced by the external field and the defects. The existence of a large difference between the local and average fields in perovskites is well known [19–21].

By differentiating (14) and (15) with respect to P_0 and $\langle S^z\rangle$, respectively, one obtains

$$(\alpha(T) + bP_0^2)P_0 - \frac{\lambda}{2\mu}P_1 = E \tag{16}$$

$$\langle S^z\rangle = \frac{W_z}{2W}\tanh\frac{W}{2k_B T}. \tag{17}$$

In order to find the dielectric susceptibility we take the derivatives with respect to E:

$$(\alpha(T) + 3bP_0^2)(P_0)'_E - \frac{\lambda}{2\mu}(P_1)'_E = 1 \tag{18}$$

$$\langle S^z\rangle' = G(E)[2\mu + \lambda(P_0)'] \tag{19}$$

with

$$G(E) = \frac{f'_{W_z}}{1 - J_0 f'_{W_z}} \qquad f'_{W_z} = \frac{\Omega^2}{2W^3}\tanh\frac{W}{2k_B T} + \frac{1}{k_B T}\frac{W_z^2}{4W^2}\left(1 - \tanh^2\frac{W}{2k_B T}\right) \tag{20}$$

where $f_{W_z} = (W_z/2W)\tanh(W/2k_BT)$. From equations (18) and (19) one easily obtains the soft mode susceptibility

$$\varepsilon_0\chi_0 = (P_0)' = \frac{1 + 2\lambda n_2\mu G(E)}{\alpha(T) + 3bP_0^2 - \lambda^2 n_2 G(E)}. \tag{21}$$

At low impurity concentrations one may neglect J_0 in equation (20), since a large distance separates the impurities. In zero field and at temperatures larger than Ω/k_B one obtains $G \approx 1/k_BT$. Hence the impurity correction of the susceptibility vanishes at large temperatures. It implies that this correction is important only at comparatively small temperatures. Obviously this correction leads to softening the critical mode.

The contribution to the dielectric susceptibility originating from the dipole impurities is

$$\varepsilon_0\chi_1 = 2\mu n_2\langle S^z\rangle' = 2\mu n_2 G(E)\frac{2\mu + \lambda(\alpha(T) + 3bP_0^2)^{-1}}{1 - \lambda^2 n_2 G(E)(\alpha(T) + 3bP_0^2)^{-1}}. \tag{22}$$

From the denominator in equation (22) it is seen that the interaction of the impurities with the soft mode strongly enhances the polarizability connected with the dipole impurities. It is particularly large in paraelectrics close to the ferroelectric phase transition, because, at $T \to T_c$, $\alpha(T) \to 0$, as discussed previously by Vugmeister and Glinchuk [22].

Finally, by summing both contributions the general expression may be derived:

$$\chi = \chi_0 + \chi_1 = \frac{1}{\varepsilon_0}\frac{1 + 4\lambda n_2\mu G(E) + 4\mu^2 n_2 G(E)(\alpha(T) + 3bP_0^2)}{\alpha(T) + 3bP_0^2 - \lambda^2 n_2 G(E)}. \tag{23}$$

It follows from this expression that the soft mode and spin coordinates influence each other rather strongly near to the ferroelectric phase transition. Only when the soft mode frequency is not too low is it possible to separate these contributions to the dielectric susceptibility.

In order to evaluate equation (23) we consider simplifications. We neglect both the interaction, $J_0 = 0$, which appears reasonable in the low impurity concentration limit, and tunnelling of the dipoles, $\Omega = 0$, thus anticipating the fact that the dipoles are of mesoscopic size due to statistical clustering (see section 2.3). Equations (16)–(20) are then reduced to

$$G(E) = \frac{1}{4k_BT}\left(1 - \tanh^2\frac{2\mu E + \lambda P_0}{2k_BT}\right) \tag{24}$$

$$[\alpha(T) + bP_0^2]P_0 - \frac{1}{2}\lambda n_2 \tanh\frac{2\mu E + \lambda P_0}{2k_BT} = E. \tag{25}$$

Equation (25) implies that the impurity contribution to the susceptibility yields some effective dependences of the linear susceptibility and the non-linearity constant on both electric field and temperature. However, it is not advised to expand the dipole contribution into a series, in the same way as the contribution originating from the host lattice. As mentioned above this procedure fails already for intermediate electric fields due to the strong non-linearity of the tanh function.

Figure 4 shows the comparison between the experimental results of χ^{-1} against T for SCT with $x = 0.07$ in zero external field, hence, $P_0 = 0$ at $T > T_c \approx 18$ K [23], and the best fit to equation (23) in connection with equation (24), $G(E) = 1/(4k_BT)$, using $\lambda = 8 \times 10^{-21}$ V m^2. Quantitative agreement is observed for $24 < T < 60$ K. However, as will be shown below this value of λ is much too small. Better agreement between theory and experiment is obtained with a realistic value of λ. It is two orders of magnitude larger while assuming that only a part of the Ca impurities are in the dipole state. Within a percolation approach it will be shown that this part depends on temperature. Figure 5 shows the tendency in the dependence of the reverse susceptibility on the concentration n_2. Obviously, the slope of the reverse susceptibility increases when the concentration is enlarged.

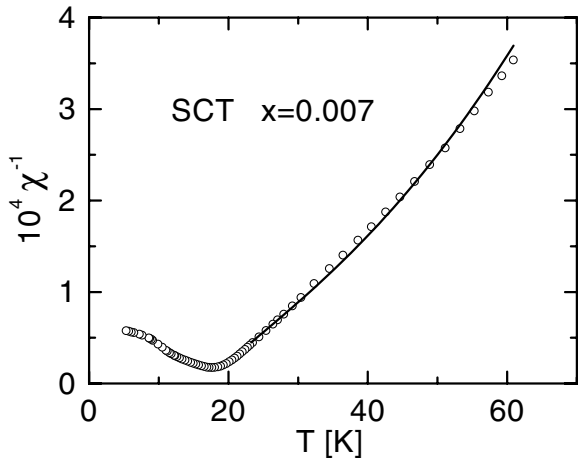

Figure 4. Temperature dependence of the inverse dielectric in-plane susceptibility [9] of SCT with $x = 0.007$ best-fitted to equation (23) for $P = 0$ and $E = 0$ at $T > T_c = 18$ K.

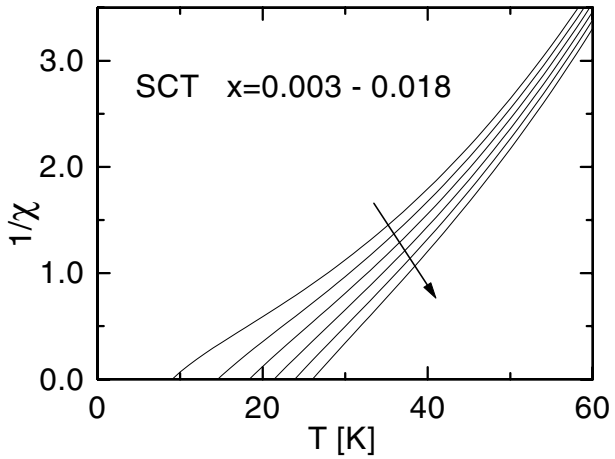

Figure 5. Temperature dependence of the inverse dielectric in-plane susceptibility [9] calculated from equation (23) for $P = 0$ and $E = 0$ with the best-fit parameters obtained for SCT with $x = 0.007$ (figure 4) for various impurity concentrations, $x = 0.003$–0.018.

Figure 6 (dashed curve) shows the result of fitting equation (23) to the experimental data [23] χ' against E (circles) on SCT with $x = 0.007$ at $T = 20$ K. To this end equations (24) and (25) have been solved and inserted self-consistently. When keeping the dipole moment at the fixed value $\mu = 10^{-30}$ mC, which corresponds to a displacement of the Ca^{2+} ion by 5 pm, we obtain the best-fit parameters $b = 2.0 \times 10^{10}$ J m^5 C^{-4} and $\lambda = 8 \times 10^{-21}$ V m^2. The latter value was also found from the best fit of χ against T (figure 4; see above), where we have already mentioned above that it appears too small. Moreover it does not change appreciably, if one enlarges μ a few times.

The fit can be improved, if one assumes that only a part of the Ca ions has a dipole moment. Probably this is just that part which forms the clusters introduced previously [5, 9] (see also section 2.3). The remaining Ca ions are assumed to influence the susceptibility as soft oscillator impurities as described in section 2.1. To this end one may simply replace the

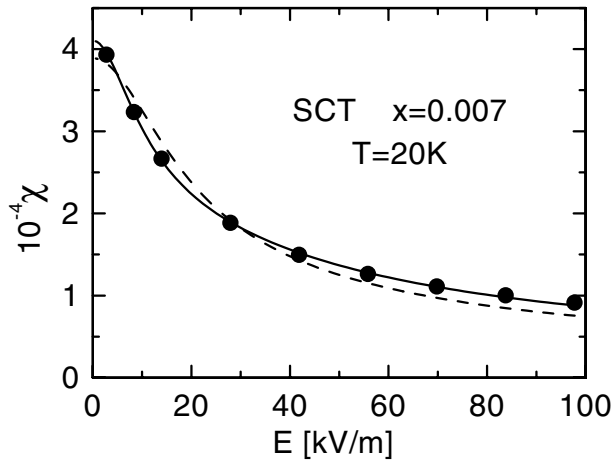

Figure 6. Electric field dependence of the dielectric in-plane susceptibility of SCT with $x = 0.007$ (solid circles [9]) best-fitted to equations (23) and (26) (dashed and solid curves, respectively; see text).

value of $\alpha(T)$ obtained for pure $SrTiO_3$ by the value $\alpha(T) - \Lambda n_1$ where n_1 is the concentration of the Ca ions in the non-dipolar state. One finally obtains

$$\chi = \frac{1}{\varepsilon_0}\frac{1 + 4\lambda(n_2 + n_{20})\mu G(E) + 4\mu^2(n_2 + n_{20})G(E)(\alpha(T) - \Lambda(n_1 + n_{10}) + 3bP_0^2)}{\alpha(T) - \Lambda(n_1 + n_{10})_1 + 3bP_0^2 - \lambda^2(n_2 + n_{20})G(E)} \tag{26}$$

where n_{10} and n_{20} are the concentrations of monopole and dipole-type impurities in the nominally pure sample, while n_1 and n_2 refer to the Ca doping in SCT. For sake of simplicity universal coupling constants Λ and λ are assumed for both kinds of impurity. Figure 6 (solid curve) shows the best fit of equation (26) to χ' against T under this assumption. It is seen that this fit is much better than the previous one (dashed curve) when choosing $b = 1.27 \times 10^{10}$ J m^5 C^{-4}, $n_2 + n_{20} = 8.74 \times 10^{-6}$ per unit cell volume, $\chi_0 = [\varepsilon_0(\alpha(20\text{ K}) - \Lambda(n_1 + n_{10}))]^{-1} = 2.5 \times 10^4$ and $\mu = 1.47 \times 10^{-29}$ C m. The value of the coupling constant, $\lambda \approx 1.11 \times 10^{-19}$ V m^2, was found from the expression $\lambda = \gamma\mu/3\varepsilon_0$, where $1/3\varepsilon_0$ is the Lorentz correction coefficient, which signifies the difference between the local and average fields in the simple cubic lattice. γ gives the correction for the local field in the perovskite-type lattice. Here we adopted the value $\gamma = 0.2$ of the Li site in $KTaO_3$ [20] to the Ca site in $SrTiO_3$.

Our fit shows that only a comparatively small part of the Ca ions are in the dipole state, while the value of the dipoles appears considerably enhanced. However, instead of conjecturing enhanced off-centre displacements of the Ca ion ($d = 46$ pm, if $q = 2e$), we rather suppose that groups of Ca ions form clusters, which are strongly correlated and collectively influence the lattice dynamics. Section 2.3 is devoted to finding reasons for such a type of clustering.

Here we would like to stress that the main reason for the rather steep decay of the dielectric susceptibility in weak electric fields is the interaction of the soft mode with the dipoles. The shift of the squared soft-mode frequency is electric field dependent due to the strong non-linearity in the dipole subsystem. This is seen from the denominator in equation (21), which contains the strong dependence of G on E. At large E the value of G vanishes and practically only the lattice is responsible for the dynamics. However at intermediate electric fields, $E \approx 10\,\text{kV m}^{-1}$, giant influence of the dipoles is encountered. Probably their influence has to be taken into account

even for nominally pure samples, since we have found above that a cluster concentration of about 10^{-5} per unit cell has already a drastic influence on the lattice dynamics.

Equation (23) does not account for dynamic effects. Indeed the frequency dispersion of the permittivity of SCT is weak above T_c [9]. This might be different in other systems and can be accounted for within the framework of the kinetic equation of the dipoles [7] (see appendix A).

2.3. Cluster formation in SCT

In order to study the possible nature of the cluster formation in SCT we employed a percolation-type technique [24]. We consider the Ca ions to be surrounded by spheres of the correlation radius $r_c = \rho\sqrt{\chi}$. The constant ρ was determined for pure $SrTiO_3$ from the correlation radius, $r_c = 2.4$ nm, obtained from the phonon spectrum of $SrTiO_3$ at low T [25]. As the dielectric susceptibility is temperature dependent the correlation radius proves to be temperature dependent too.

By using a random number generator we distributed the Ca^{2+} impurities over the lattice sites in cubes of size 480^3 for $x = 0.002$ and 120^3 for $x = 0.007$. Weakly correlated clusters were defined by the condition of mutual intersection of individual correlation spheres, $r \leqslant r_c$, where $2r$ is the distance between two Ca impurities. Alternatively, strongly correlated clusters were defined in the same way, however, by reducing the correlation radius considerably, $r \ll r_c$. When choosing $r = 0.02r_c$ the percolation threshold appears just at the temperature of the phase transition for $x = 0.007$ (see below). For each realization of the impurity distribution we computed the average size of the cluster defined by [26]

$$\langle S\rangle = \sum_i s_i w_i = \sum_i s_i s_i \Big(\sum_j s_j\Big)^{-1} = \Big(\sum_i s_i^2\Big)\Big(\sum_i s_i\Big)^{-1}. \tag{27}$$

Here s_i is the number of impurities in the ith cluster. The connected cluster, containing the number of s_{inf} impurities, spreads from one side (say from the bottom of the cube) to the opposite one and defines the order parameter $P_{inf} = s_{inf}/\sum_i s_i$.

Figures 7(a) and (b) show the results of the computation of the order parameter P_{inf} and the average cluster size $\langle S\rangle$ after ensemble averaging over 10^3 realizations. The data have, hence, a relative accuracy not worse than 10^{-3}. It is seen that both the onset temperatures of long-range order for weakly correlated clusters (curves labelled as 1), viz. $P_{inf} > 0$ at $T_c(x = 0.002) \approx 15$ K, $T_c(x = 0.007) \approx 120$ K (solid lines) and the peak temperatures of cluster sizes ($\langle S\rangle_{max}$; dashed lines) are much too high when compared to the measured ones [5] $T_c(x = 0.002) \approx 0$ K, $T_c(x = 0.007) \approx 18$ K. However, those referring to strongly correlated clusters for $x = 0.007$ (curves labelled as 2 in figure 7(b)) meet exactly the experimental experience, while for $x = 0.002$ the threshold is completely absent. It implies that clustering appears only at the comparatively large Ca concentration, $x = 0.007$ whereas it is practically absent for $x = 0.002$. It should be noticed that the final criterion for a global phase transition is provided by the vanishing of the denominator in equation (26).

It should be noticed that spontaneous symmetry breaking of the impurities has tacitly been assumed within the correlated clusters, although they might consist of centrosymmetric soft impurities. In this case an interaction mechanism has to be found explaining the global symmetry breaking. This is attempted in appendix B by assuming linear coupling between nearby anharmonic oscillators.

In conclusion we like to stress that the two models presented in this paper must very probably not considered as alternative solutions, but as complementary ones. Both contributions to the dielectric behaviour of SCT are believed to contribute simultaneously,

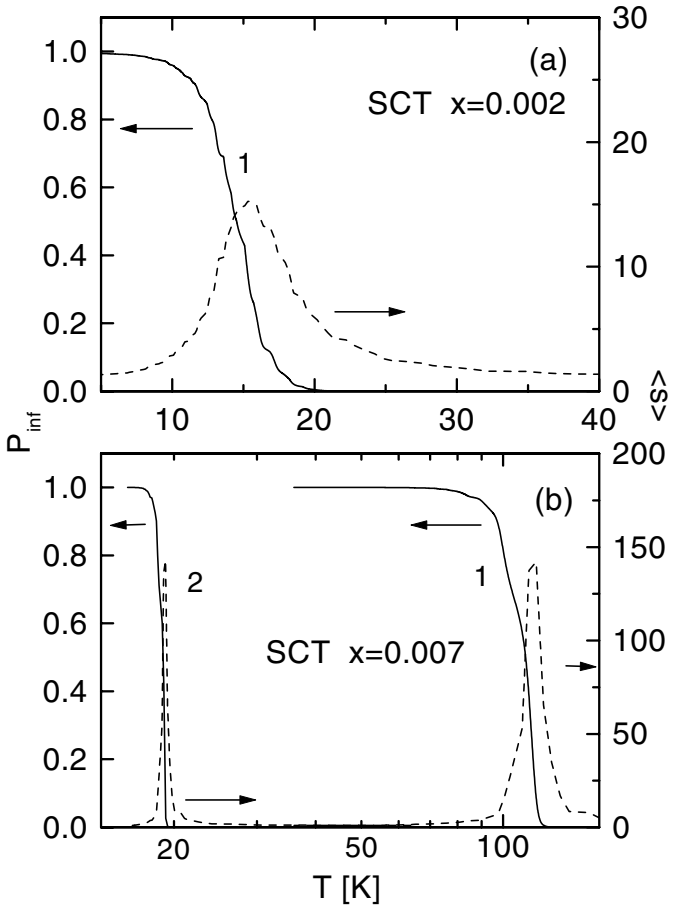

Figure 7. Temperature dependences of average cluster size $\langle S \rangle$ (broken curves) and order parameter P_{inf} (solid curves) in SCT with $x = 0.002$ (a) and 0.007 (b) for weakly (curves 1) and strongly correlated clusters (curves 2 in (b)), respectively (see text).

those stemming from dipoles and those from soft oscillators. Isolated Ca^{2+} ions substituted at Sr^{2+} sites are certainly not rigid dipolar entities owing to the low trapping potential of possible off-centre configurations. This changes at high enough Ca^{2+} concentrations, where mutual interaction breaks the spherical symmetry of the impurities and finite dipole moments are induced as shown in appendix B.

3. Conclusion

We have developed a theory of dielectric response of quantum paraelectric $SrTiO_3$ doped with Ca. The impurities are thought to be in two possible states, dipole and monopole. While the monopole impurities soften the ferroelectric soft mode due to lower spring constants of the Ca–O bonds when compared to those of Sr–O, the dipole-type Ca impurities give rise to further softening of the lattice modes through local field effects. These result in coupling of the dipole coordinates to the soft mode displacement. According to numerical analysis of experimental data for SCT with $x = 0.007$ the number of dipolar impurities is relatively low, but it grows

with decreasing temperature. This complies with the idea that groups of Ca impurities are forming dipolar clusters, whenever their correlation spheres mutually overlap. Percolation model computations are in rough agreement with such a supposition.

We have stressed that the small fraction of dipolar Ca impurities saturates at relatively weak electric field. Hence, their contribution to the dielectric susceptibility rapidly vanishes when increasing E. Owing to its quantum nature this part of the response function cannot be described by a low-order series expansion. This explains the previous failure of describing χ against E in the conventional way. Very probably this dipolar contribution is also responsible for the well known relaxor properties of SCT [5]. Indeed, only a small subsystem of the crystal seems to be responsible for polydispersivity, one of the main characteristics of the relaxor system. E.g. in SCT with $x = 0.002$ only about 5% of the low-T dielectric response at $E = 0$ is polydispersive at low frequencies [27]. It will be left as a task for the future to develop a deeper understanding of the dynamics of this subsystem. As mentioned previously [26], a correlated domain model [28] might provide an adequate description. A first step towards a microscopic description is proposed in appendix A.

In conclusion we would like to stress that the two models presented in this paper must very probably not considered as alternative solutions, but as complementary ones. Both contributions to the dielectric behaviour of SCT are believed to contribute simultaneously, those stemming from dipoles and those from soft oscillators. Isolated Ca^{2+} ions substituted at Sr^{2+} sites are certainly not dipolar entities owing to the low trapping potential of possible off-centre configurations. This changes at high enough Ca^{2+} concentrations, where mutual interaction breaks the spherical symmetry of the impurities and finite dipole moments are induced as shown in appendix B.

Acknowledgments

JD and SAP are grateful to the Deutsche Forschungsgemeinschaft for financial support and for the hospitality of the Laboratorium für Angewandte Physik during their stay at GMU Duisburg.

Appendix A. Dispersion of the dielectric susceptibility

The final expression, equation (23), of the susceptibility does not take into account dispersion effects, since we know from the experiment that they are weak above T_c. However for the sake of generality and in order to make our expression applicable to materials with noticeable dispersion, an appropriate expression will be derived here.

The starting point for our derivation is the kinetic equation of the dipoles [7]

$$\mathrm{i}\hbar\frac{\mathrm{d}\rho_d}{\mathrm{d}t} = [H_d\rho_d] - \frac{\mathrm{i}\hbar}{\tau}(\rho_d - \overline{\rho}_d) \tag{A.1}$$

where ρ_d is the density matrix for the dipole subsystem, $\overline{\rho}_d$ is the statistically averaged density matrix for each value of the local field, τ is the relaxation time and H_d is the part of the Hamiltonian (13) connected with the dipoles. After carrying out the Fourier transformation one obtains a final expression for the dielectric susceptibility, which has the form of equation (23) with $G(E)$ defined by (20) but with a new expression for f'_{W_z},

$$f'_{W_z} = \frac{1}{(1+\mathrm{i}\omega\tau)}\left\{\frac{\Omega^2}{2W^3}\tanh\frac{W}{2k_BT} + \frac{W_z^2}{4W^2k_BT}\frac{1}{\cosh^2(W/2k_BT)}\right\}. \tag{A.2}$$

In comparison with equation (20) it is seen that the only new feature is a factor depending on frequency and standing in front of the brackets. This result generalizes also an expression derived in [29] by taking into account tunnelling, inter-dipole interactions and polarization.

Appendix B. Symmetry breaking in soft impurity pairs

In our percolation treatment we assumed that the soft impurities being close each other are symmetry broken. Hence, these impurities have dipole moments, which are strongly correlated within the cluster as expressed by the term 'cut-off radius'. However, the thermodynamics of symmetry breaking needs to be clarified. Here we show how a model recently proposed by Perez-Mato and Salje [30] might be applied to this situation.

We start with a two-impurity Hamiltonian

$$H = \frac{p_1^2}{2M} + \frac{M\omega_0^2}{2}x_1^2 + \frac{p_2^2}{2M} + \frac{M\omega_0^2}{2}x_2^2 + \frac{1}{4}ux_1^4 + \frac{1}{4}ux_2^4 - zx_1E - zx_2E - \frac{1}{2}\upsilon x_1x_2 \tag{B.1}$$

with the conventional meaning of the constants involved. The trial Hamiltonian is of the form [30]

$$H_0 = \frac{p_1^2}{2M} + \frac{M\omega^2}{2}(x_1 - x)^2 + \frac{p_2^2}{2M} + \frac{M\omega^2}{2}(x_2 - x)^2. \tag{B.2}$$

Here x is the average displacement in the selected pair. Notice that this displacement has nothing to do with the macroscopic order parameter, since no interactions among different impurity pairs are involved in the considered model (they are at least weaker than those between the paired ions).

By treating this Hamiltonian in the same manner as in [30] one obtains that symmetry breaking appears under the condition

$$2M\omega_0^2 + 6\sigma(T) - \upsilon(R) < 0 \tag{B.3}$$

where $\sigma = (\hbar/2M\omega)\coth(\hbar\omega/2k_BT)$ is the variance. While $\overline{x} = 0$ above the critical temperature (which is, in principle, different for different pairs as they are at different distances, R), one has $\overline{x}^2 = -(2M\omega_0^2 + 6\sigma(T) - \upsilon(R))/2u$ below T_c.

At the bifurcation point $\overline{x}$ depends on T as $\sqrt{T_c(R) - T}$, while it saturates at low T due to zero-point quantum vibrations of the Ca impurities. Upon increasing the distance between the impurities $T_c(R)$ decreases. Hence, at a fixed temperature, there exists a largest distance, R_c, at which the local symmetry breaking appears ($T = T_c(R_c)$). However, there exists a distance, R_0, beyond which symmetry breaking will never occur because of the quantum vibrations ($T_c(R_0) = 0$), even if $2M\omega_0^2 - \upsilon(R) > 0$. This happens because the quantum variance $\sigma(T)$ does not vanish at zero temperature in contrast to the classic one.

References

[1] Müller K A and Burkard H 1979 *Phys. Rev.* B **19** 3593
Müller K A 1985 *Japan. J. Appl. Phys.* **24** (Suppl. 24-2) 89
[2] Uwe H and Sakudo T 1977 *Phys. Rev.* B **15** 337
[3] Bednorz J G and Müller K A 1984 *Phys. Rev. Lett.* **52** 2289
[4] Dec J, Kleemann W, Bianchi U and Bednorz J G 1995 *Europhys. Lett.* **29** 31
[5] Kleemann W, Dec J, Wang Y G, Lehnen P and Prosandeev S A 2000 *J. Phys. Chem. Solids* **61** 167
[6] Born M and Huang K 1954 *Dynamical Theory of Crystal Lattices* (Oxford: Clarendon)
[7] Vaks 1973 *Vvedenie v Mikroskopicheskuiu Teoriju Segnetoelektrikov* (Moscow: Nauka) (in Russian)
Prosandeev S A, Kleemann W and Dec J 2001 *Integrated Ferroelectr.* **32** 287
[8] Hayward S A and Salje E K H 1998 *J. Phys.: Condens. Matter* **10** 1421
[9] Kleemann W, Dec J and Westwanski B 1998 *Phys. Rev.* B **58** 5985
Dec J, Kleemann W and Westwanski B 1999 *J. Phys.: Condens. Matter* **11** L379
[10] Vogt H 1995 *Phys. Rev.* B **51** 8046
[11] Blinc R and Zeks B 1974 *Soft Modes in Ferroelectrics and Antiferroelectrics* (Amsterdam: North-Holland)
[12] Rechester A B 1971 *Zh. Eksp. Teor. Fiz.* **60** 782
[13] Migoni R, Bilz H and Bäuerle D 1976 *Phys. Rev. Lett.* **37** 1155

[14] Bäuerle D, Wagner D, Wöhlecke M, Dorner B and Kraxenberger H 1980 *Z. Phys.* B **38** 335
[15] Sirenko A A, Bernhard C, Golnik A, Clark A M, Hao J-H, Si W and Xi X X 2000 *Nature* **404** 373
[16] Smolyaninov L M and Glinchuk M D 1998 *J. Korean Phys. Soc.* **32** S400
[17] Maglione M 1996 *Ferroelectrics* **176** 1
[18] Kleemann W, Dec J, Prosandeev S A and Wang Y G 2000 *Ferroelectrics* **239** 257
[19] Slater J C 1950 *Phys. Rev.* **78** 748
[20] Prosandeev S A and Riabchinskii A I 1996 *J. Phys.: Condens. Matter* **8** 505
[21] Turik A V 1993 *Izv. AN SSSR* **57** 35
[22] Vugmeister B E and Glinchuk M D 1990 *Rev. Mod. Phys.* **62** 993
[23] Bianchi U, Dec J, Kleemann W and Bednorz J G 1995 *Phys. Rev.* B **51** 8737
[24] Stauffer D and Aharony A 1992 *Introduction to Percolation Theory* (London: Taylor and Francis)
[25] Prusseit-Elffroth W and Schwabl F 1990 *Appl. Phys.* A **51** 361
[26] Gould H and Tobochnik J 1988 *An Introduction to Computer Simulation Methods: Applications to Physical Systems* (Reading, MA: Addison-Wesley)
[27] Kleemann W, Albertini A, Chamberlin R V and Bednorz J G 1997 *Europhys. Lett.* **37** 145
[28] Chamberlin R V 1998 *Phase Transitions* **65** 169
[29] Girshberg Y and Yacoby Y 1999 *J. Phys.: Condens. Matter* **11** 9807
[30] Perez-Mato J M and Salje E K H 2000 *J. Phys.: Condens. Matter* **12** L29